ACS SENSORS

pubs.acs.org/acssensors

Letter

Moving Electrode Impedance Spectroscopy for Accurate Conductivity Measurements of Corrosive Ionic Media

Nikolaus Doppelhammer,* Nick Pellens, Johan Martens, Christine E. A. Kirschhock, Bernhard Jakoby, and Erwin K. Reichel

Cite This: *ACS Sens.* 2020, 5, 3392–3397

Read Online

ACCESS | Metrics & More | Article Recommendations | Supporting Information

ABSTRACT: A measurement cell for the use of accurate conductivity measurements of corrosive ionic media is presented. Based on the concept of moving electrode electrochemical impedance spectroscopy, exceptional measurement accuracy is achieved in a large conductivity range. Extensive testing with corrosive ionic media demonstrated the robust operation of the cell under harsh chemical conditions, up to temperatures of 130 °C. The novel design allows monitoring small conductivity changes during chemical reactions in ionic media, for instance, zeolite formation from hydrated ionic liquids.

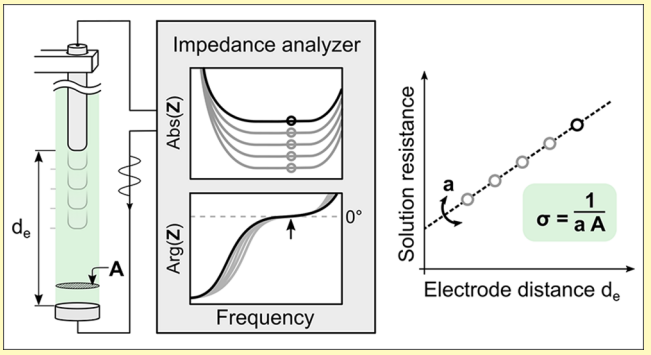

KEYWORDS: *conductivity, cell design, electrochemical impedance spectroscopy, adjustable electrode distance, corrosive media, ionic liquids, high accuracy*

Conductivity measurements are commonly used for monitoring and characterization of electrolyte solutions with applications in fuel cells,[1,2] water quality management,[3,4] and Bayer[5,6] and chlor-alkali[7] process monitoring. Thorough analysis of such conductivity measurements provide insight into complex molecular-scale processes, such as ionic association dynamics in ionic liquids,[8,9] reaction kinetics in (electro)chemical processes,[10−12] or formation of zeolites.[13] For such advanced applications, it is beneficial to use a high-accuracy conductivity measurement cell, capable of measuring in a wide conductivity range and which is resistant to a broad spectrum of corrosive ionic media.

Most commonly, two types of conductivity sensors are used: electrode-based sensors and inductive sensors. Electrode sensors are suitable for low and moderate conductivities, with accuracies between ±3% and ±5% in the conductivity range from 2×10^{-8} to 0.65 S cm^{-1}.[14,15] In common devices, the accuracy decreases due to the compact design of these sensors, especially toward higher conductivities. Moreover, in reactive media, electrode fouling can alter the cell constant with negative impact on measurement accuracy.

Inductive conductivity sensors are especially suitable for harsh chemical environments because only inert and heat-resistant materials, such as PEEK and PTFE, are in contact with the sample. However, these sensors lack the sensitivity of their electrode-type counterparts and require large sample volumes.[16] The latter is disadvantageous in laboratory applications, for instance, when space is limited or when large sample series need to be analyzed. Because of the above reasons, we argue that a conductivity measurement cell for broad applicability of high-accuracy measurements of corrosive ionic media with small sample volumes is lacking, which obstructs progress in the implementation of advanced conductivity observation for the mentioned scientific areas.

Cell Design. The cell design is illustrated in Figure 1. The main feature is a long counter electrode which is mounted on a motorized linear stage to accurately control its vertical position. The linear stage is a Thorlabs LTS300/M with a position accuracy of 3.89 μm. The counter electrode is introduced into an elongated PTFE tube that contains the sample. The working electrode is located at the bottom of the setup and mounted on the sample tube by means of a silicone O-ring. Due to the elongated design of the cell, large electrode distances are achievable. The sample tube is enclosed by a brass housing, which is connected to a thermostatic bath. A PT100 temperature sensor is mounted next to the sample tube to control the sample temperature (Supporting Information). All wetted parts are entirely made of corrosion- and heat-resistant materials, such as PTFE, PEEK, and silicone.

Received: July 16, 2020
Accepted: October 19, 2020
Published: October 27, 2020

https://dx.doi.org/10.1021/acssensors.0c01465
ACS Sens. 2020, 5, 3392–3397

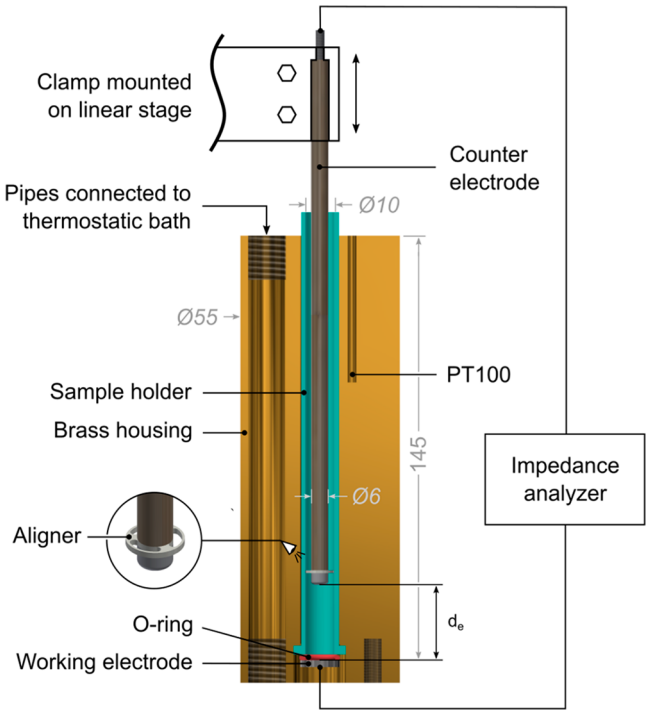

Figure 1. Design of the moving electrode conductivity cell. All dimensions in mm.

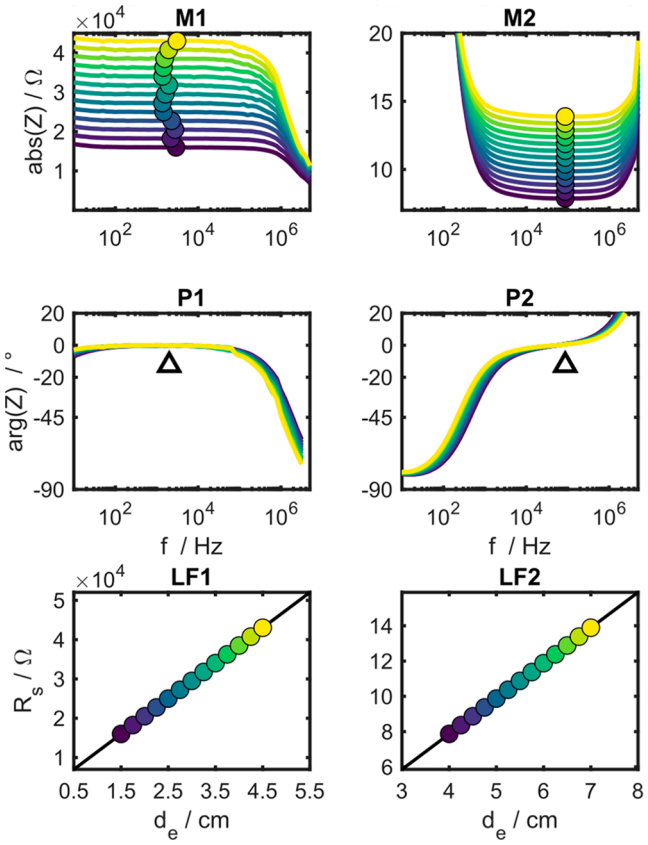

Figure 2. MEEIS impedance spectra (magnitude (M) and phase (P)) and solution resistance as linear functions of the electrode distance (LF) for two test liquids with low (1) and high (2) conductivity (σ_1 = 1.38 × 10^{-4} S cm^{-1}, σ_2 = 0.625 S cm^{-1}). Each circle represents the mean of the ten impedance values with the closed phase angle to zero. The triangles indicate at which frequency arg(Z) is minimal. For both cases, we obtained a highly accurate fit with slopes a_1 = 9007 ± 6.59 Ω cm^{-1} and a_1 = 2.0058 ± 0.0013 Ω cm^{-1} (black lines in LF1 and LF2, respectively). The slope is directly related to the conductivity via eq 1.

Titanium grade 2 is used as electrode material, a metal which is known for excellent corrosion resistance in various ionic media. The working and counter electrodes are connected to a capable potentiostat that collects data. Operation of the whole setup was automated in Python.

Data Acquisition and Processing. High measurement accuracy is achieved utilizing a novel method called moving-electrode electrochemical impedance spectroscopy (MEEIS). The principle of MEEIS, presented earlier to analyze the sedimentation behavior of particles in conductive suspensions,[17] and was revised and optimized in this work for high-precision conductivity measurements.

The design meets the requirement to record impedance spectra over a large frequency range for various electrode distances d_e, as shown in the magnitude and phase plots in Figure 2 for the cases of a highly (M1 and P1) and a poorly (M2 and P2) conductive test liquid. EIS spectra of liquid samples are generally interpreted using equivalent circuit models. With an appropriate model, parameters such as the double-layer capacitance, the charge transfer resistance, or the bulk conductivity can be determined.[18] As we are interested solely in bulk conductivity, it is possible to exploit the principle of MEEIS to provide a more efficient and robust data analysis. We found that the change in impedance for measurements with negligible capacitive and inductive contributions (arg(Z) ∼ 0°) varies strictly linearly with the electrode distance d_e and can be approximated by a linear function, as illustrated in Figure 2 (LF1 and LF2). If a denotes the slope of this function, the conductivity can be directly expressed as

$$\sigma = \frac{1}{aA} \tag{1}$$

with A being the effective cross section of the sample. the cross section of the sample tube. In our setup, the value of A = 0.7976 ± 0.002 cm^2 was determined via calibration with a conductivity standard and corresponds to the actual cross section of the sample tube. Equation 1 shows that the conductivity depends solely on the linear fit parameter a and not on the sample length. This is a key difference to static cells, where electrode distance and cross section cannot be determined separately, but always appear in a single term denoted as the cell constant $c = l/A$. As discussed in our previous work,[17] this invariance of the sample length allows independent investigation of electrode(-near) and bulk effects, which, for instance, is useful for studying samples that tend to phase separate.

Depending on the sample properties, the region of negligible capacitive (arg(Z) < 0°) and inductive effects (arg(Z) > 0°) shifts drastically, as visible in the phase diagrams in Figure 2 (P1 and P2). This requires selective frequency adaption to determine the value of a correctly. In contrast to equivalent circuit modeling, our approach allows effortless automation without any prior information on the sample properties, as demonstrated by automated data analysis in Python 3.8.2. Further experimental details such as measurement voltage used, frequency range, etc. are provided in the Supporting Information.

https://dx.doi.org/10.1021/acssensors.0c01465
ACS Sens. 2020, 5, 3392−3397

Solution Resistance at Small Electrode Distances. Earlier, we demonstrated that the linear relationship between electrode distance and sample resistance is valid for large electrode gaps.[17] However, this linear relationship is lost when the distance between the electrodes becomes too small. To investigate where the linear behavior ends, computer simulations using the Finite Element software COMSOL were performed and a cell with similar geometry was designed based on the setup shown in Figure 1 (Supporting Information).

We simulated the current density field inside the sample to spot regions of nonuniform current distribution and to investigate how the field changes when the electrode distance is varied. If the current is distributed nonuniformly across the sample cross section, as can be the case near the electrodes, it will contribute a larger fraction of the overall sample resistance. A linear change of this parameter can therefore only be expected if the current density field is not distorted when the electrode distance is varied.

As evident from the results in Figure 3, the electrode geometry G1 preserves a uniform current density distribution, even at small electrode distances. The situation changes when a different electrode design is chosen. For geometries G2 and G3, field distortions were much more pronounced when the electrodes were approaching closely, indicating an early end of the linear resistance regime. The trends evident in the field plots were confirmed by computing the solution resistances between the electrode surfaces from the current−density fields as functions of the electrode distance. The results are presented in Figure 4. As expected, we see that the solution resistance increased linearly with the electrode distance for design G1, whereas for G2 and G3 a nonlinear behavior was observed at small electrode distances. The largest change in resistance was observed for G3, where electrodes with a small surface area were used, followed by G2 and then G1. Interestingly, all geometries transited into the same linear behavior (same slope), once the electrode distance became sufficiently large. This behavior was further experimentally confirmed by using different counter electrode geometries (Supporting Information) and demonstrates an important aspect of MEEIS in its practical application. Under the assumption that the electrode properties do not change during data acquisition (e.g., due to fast corrosion of the electrode surface), the conductivity determined by MEEIS is independent of the electrode properties and geometry. This means that electrodes can be changed without the need for recalibration, and long-term passivation effects on the electrode surfaces do not influence the measurement. This is a major advantage over electrode sensors with nonmovable electrodes, where electric decoupling of electrode(-near) and bulk effects is impossible and a change of, i.e., the electrode surface area alters the cell constant.[19] Bubbles on the sidewalls, which might locally decrease the sample cross section, are not an issue, as they are wiped off by the aligning element shown in Figure 1. This feature was automated in the data acquisition program and is executed just before data acquisition starts.

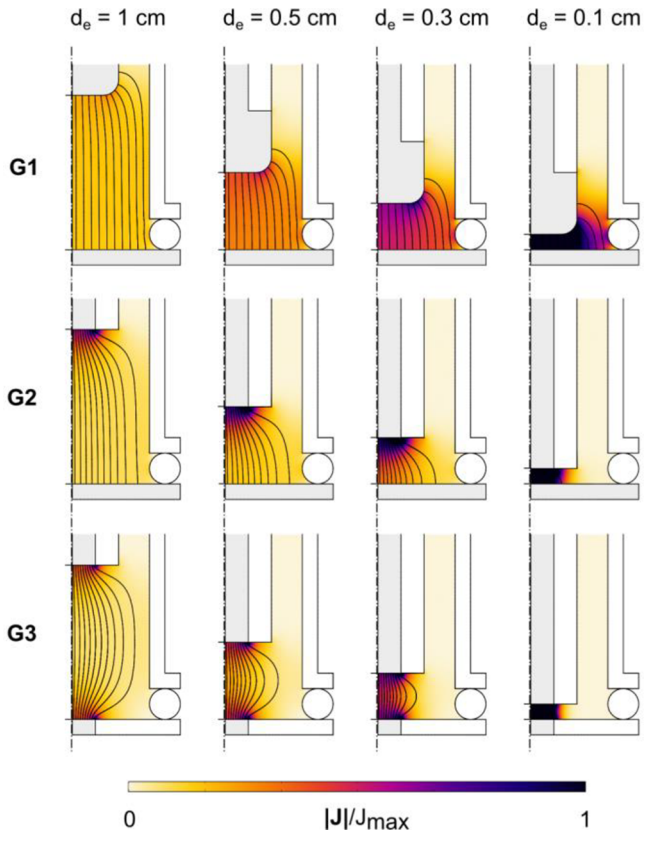

Figure 3. 2D axisymmetric simulations of the current−density distribution for three electrode designs at small electrode distances. Gray parts are electrodes, and white parts are modeled as insulators.

Influence of Nonuniform Temperature Distribution. The electrical properties of liquid samples are temperature-dependent, especially for concentrated electrolytes. The conductivity of concentrated potassium hydroxide solutions, for instance, changes by up to 1%/°C.[20] For organic EMIM-based ionic liquids, a maximum change of 1.4%/°C was reported.[21]

The thermostatic bath controller used has a temperature stability <0.01 °C. Since the temperature is sensed locally at one point outside the sample, the extent to which the temperature differs inside the sample remains elusive. To investigate this aspect, we replaced the counter electrode by a precision reference thermometer and analyzed the temperature inside the sample at several vertical positions. We found that for electrode distances d_e > 1.5 cm, a temperature stability <0.1 °C was achieved for all adjusted set point temperatures (40, 60, and 80 °C). For smaller electrode distances, deviations became larger and more pronounced, especially at higher temperatures,

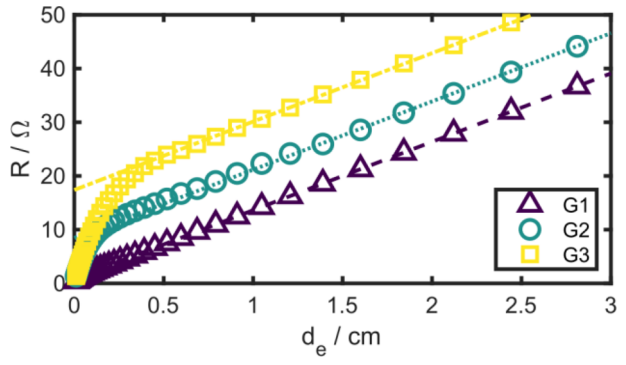

Figure 4. Sample resistance as a function of the electrode distance for simulated electrode geometries in Figure 3. The line fit was calculated for data points in the linear region (data points between 3 and 6 cm not shown).

https://dx.doi.org/10.1021/acssensors.0c01465
ACS Sens. 2020, 5, 3392−3397

as illustrated in Figure 5. The greatest deviation of ΔT = 1.5 °C was found at d_e = 0 cm at a set point temperature of 80 °C. In practice, temperature gradients near the working electrode do not affect the conductivity measurement for the following reason: As already discussed in our previous work,[17] MEEIS measures the sample only between the smallest and largest adjusted electrode distance. If sufficiently large electrode distances are chosen, as required for moderately and highly conductive samples, effects near the working electrode do not affect the conductivity measurement.

Measurement Accuracy and Conductivity Range. As proposed, an important quality feature of our cell is its high accuracy for a large bandwidth of conductivities measured. In theory, the electrolytic conductivity does not influence measurement accuracy. The impact of the electromagnetic skin effect can be excluded in the frequency range of interest due to the relatively low conductivities of ionic solutions compared to those of metals. In practice, however, high accuracy is guaranteed only when the recorded impedances are within the limitations of the measurement hardware.

To investigate this aspect, we performed room-temperature experiments with KCl solutions in a broad conductivity range. Accuracy was quantified utilizing 95% confidence intervals, determined from the goodness of fit of the parameter a in eq 1 (Supporting Information). Our findings, illustrated in Figure 6, show that exceptional measurement accuracy was achieved over a wide conductivity range from 5.6×10^{-5} S cm^{-1} to 0.82 S cm^{-1} with a mean relative uncertainty of ±0.23%. The largest uncertainty of 1.37% was measured for the least conductive sample, which can be explained by the interference-prone measurement of small currents that are at the detection limit of the measurement instrumentation.

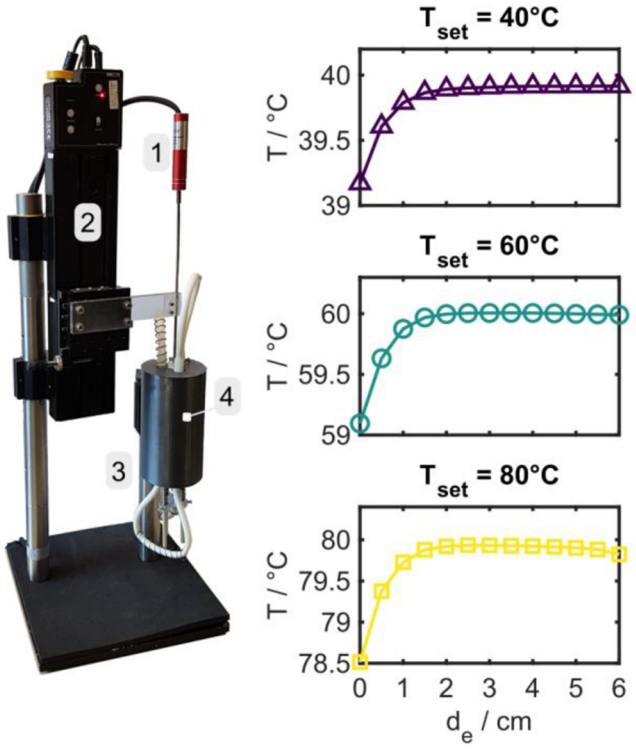

Figure 5. (Left) Setup for measuring temperature at variable electrode positions inside the sample. (1) Precision reference sensor, (2) linear stage, (3) thermally isolated cell, and (4) cell-mounted PT100 temperature sensor as shown in Figure 1. (Right) Temperature distribution for various set point temperatures and electrode distances.

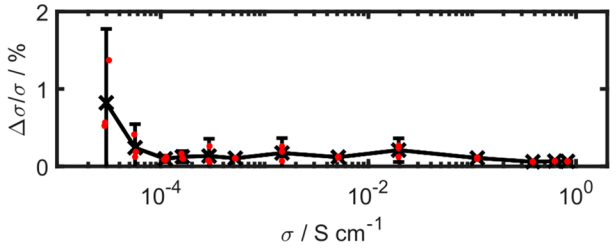

Figure 6. Relative measurement uncertainty (95% confidence interval) for solutions with various conductivities at room temperature. Error bars are drawn only for the samples measured in triplicate with the original data points shown in red.

Conductivity Measurements of Corrosive Ionic Media. Finally, we investigated the proper operation of our setup under chemically harsh conditions and at high temperatures. As ionic media, solutions of alkaline potassium hydroxide and acidic hydrochloric acid were chosen. The constituting ions of these chemicals exhibit high limiting molar conductivities (λ_{m,K^+} = 73.5, λ_{m,OH^-} = 197.9, λ_{m,H^+} = 344, λ_{m,Cl^-} = 76.3 in S cm^2 mol^{-1}), which results in high conductivity values in concentrated media. Due to extreme pH of these liquids, only a few materials exhibit proper corrosion resistance. In our setup, all wetted, nonconducting components are inert against these chemicals. The titanium electrodes have a high corrosion resistance in alkaline media but are sensitive to corrosion of some acids, such as concentrated HCl solutions.[22] Nonetheless, we used HCl solutions to show that even in this case, accurate conductivity measurements can be performed when using our moving electrode approach.

For each ionic medium, solutions of varying concentration were measured at various temperatures and compared to reference data from the literature.[20,23] As before, measurement accuracy was determined from the goodness of fit of the parameter a in eq 1. All measurement data, including errors and a comparison to reference data, can be found in Tables S1−S6 in Supporting Information.

We find that for all tested cases, measurement uncertainties are small, with average values of ±0.11% and ±0.064% for the KOH and HCl solutions, respectively. When compared to reference data, we observed that measured and reported values differed on average by about 4.09% and by a maximum of 7.48% for the 40 wt % solution at 100 °C. HCl solutions differed on average by about 1.4% and by a maximum of 2.28% for the 10 wt % solution at 25 °C. Presumably, these differences do not arise from the measurement itself but external factors. As KOH is a hygroscopic CO_2-absorbing substance, samples are easily contaminated. The observed conductivity is very sensitive to variations in the water content, especially at high ion concentrations. The latter also applies for concentrated HCl solutions. Additionally, the accuracy of published data can be questioned. In the KOH case, where data of various authors is available, the review of Gilliam et al.[20] reported differences of up to 10%.

Due to the high boiling point of KOH in the most concentrated case, we could demonstrate the proper functioning of our cell at high temperatures. Even at the highest tested temperature of 130 °C, measurement uncertainties were no larger than ±1.3%. Unfortunately, we

https://dx.doi.org/10.1021/acssensors.0c01465
ACS Sens. 2020, 5, 3392−3397

could not find existing data from the literature to compare our measurement results in this case.

Experiments with HCl demonstrated the robustness of MEEIS in harsh chemical conditions. Despite severe corrosion of the electrode surface, as shown in Figure 7, a mean measurement uncertainty of ±0.064% was achieved. This confirms the previously stated advantage of MEEIS that slow alteration of the electrode surface does not affect the measurement results. However, due to contamination of the analyte over time, we recommend choosing an electrode material which is less susceptible to corrosion. As mentioned previously, conductivity measurement using MEEIS is independent of the electrode geometry and surface condition, so electrodes can be changed without the need for recalibration.

To conclude, we have reported a setup that combines high accuracy and robust design for use in conductivity measurements of corrosive ionic media. In moving-electrode impedance spectroscopy, the conductivity is determined not from the absolute value of the sample impedance as in static cells, but from the change in sample impedance arising from varying the electrode position. By automatically selecting a suitable frequency range, conductivity is determined solely from the bulk of the sample, excluding influences of the electrode–liquid interface (double-layer), of long-term passivation of the electrode surface, and of cable or contact impedances. Various electrode geometries were simulated to find an optimal design that ensures high linearity of the solution resistance even at small electrode distances. Furthermore, we could demonstrate that, once the linear relationship between electrode distance and sample resistance is established, the conductivity measurement will be independent of the electrode geometry or its properties. Thus, alteration of electrode properties or changing the electrodes does not require recalibration of the cell. Temperature gradients inside the sample were analyzed thoroughly to determine the regions of highest measurement accuracy. Extensive testing with corrosive, ionic media showed that the relative measurement uncertainty is on average ±0.23% for conductivities in the range of 5.6×10^{-5} to 0.82 S cm^{-1}. Compared to commercially available electrode sensors, with specified accuracies as large as 3–5%,[14,15] this is a more than 10-fold increase in accuracy. Moreover, experiments with caustic solutions of potassium hydroxide and concentrated hydrochloric acid demonstrated the robust operation of our setup under chemically harsh conditions and in a large temperature range up to 130 °C.

We will use this setup to study in situ process monitoring, for instance, of the formation of zeolites from so-called hydrated silica ionic liquids.[24] These are highly alkaline liquids which form zeolites upon hydrothermal treatment at temperatures above 60 °C. The resistance changes in the solution during synthesis are expected to be small, and thus accurate conductivity measurement will be essential.

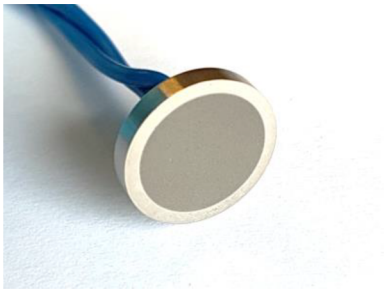

Figure 7. Titanium working electrode after severe corrosion (gray area) from experiments with concentrated HCl.

■ ASSOCIATED CONTENT

Supporting Information

The Supporting Information is available free of charge at https://pubs.acs.org/doi/10.1021/acssensors.0c01465.

List of instruments, temperature sensor calibration, calibration of the sample cross section, temperature control, measurement procedure and settings, additional information on data acquisition and processing, error analysis, current density simulations in COMSOL, experimental validation of simulation results, conductivity data of KOH and HCl experiments, and other data (PDF)

■ AUTHOR INFORMATION

Corresponding Author

Nikolaus Doppelhammer – *Institute for Microelectronics and Microsystems, JKU Linz, A-4040 Linz, Austria;* orcid.org/0000-0002-2611-9216; Email: nikolaus.doppelhammer@gmail.com

Authors

Nick Pellens – *Centre for Surface Chemistry and Catalysis: Characterization and Application Team, KU Leuven, 3000 Leuven, Belgium*

Johan Martens – *Centre for Surface Chemistry and Catalysis: Characterization and Application Team, KU Leuven, 3000 Leuven, Belgium*

Christine E. A. Kirschhock – *Centre for Surface Chemistry and Catalysis: Characterization and Application Team, KU Leuven, 3000 Leuven, Belgium*

Bernhard Jakoby – *Institute for Microelectronics and Microsystems, JKU Linz, A-4040 Linz, Austria*

Erwin K. Reichel – *Institute for Microelectronics and Microsystems, JKU Linz, A-4040 Linz, Austria*

Complete contact information is available at: https://pubs.acs.org/10.1021/acssensors.0c01465

Notes

The authors declare no competing financial interest.

■ ACKNOWLEDGMENTS

This project was funded by the bilateral Austrian Science Fund (FWF)/Research Foundation Flanders (FWO) project ZeoDirect I 3680-N34 and was supported by the "LCM – K2 Center for Symbiotic Mechatronics" within the framework of the Austrian COMET-K2 program and by long-term funding of the Flemish Government via the Methusalem program. We thank Mrs. Ingrid Abfalter, science editor on the JKU, for proofreading this work.

■ REFERENCES

(1) Lee, C. H.; Park, H. B.; Lee, Y. M.; Lee, R. D. Importance of Proton Conductivity Measurement in Polymer Electrolyte Membrane for Fuel Cell Application. *Ind. Eng. Chem. Res.* **2005**, *44*, 7617–7626.

(2) Xiao, L.; Zhang, H.; Jana, T.; Scanlon, E.; Chen, R.; Choe, E.-W.; Ramanathan, L. S.; Yu, S.; Benicewicz, B. C. Synthesis and

Characterization of Pyridine-Based Polybenzimidazoles for High Temperature Polymer Electrolyte Membrane Fuel Cell Applications. *Fuel Cells* **2005**, *5*, 287−295.
(3) Ramos, P. M.; Pereira, J. M. D.; Ramos, H. M. G.; Ribeiro, A. L. A Four-Terminal Water-Quality-Monitoring Conductivity Sensor. *IEEE Trans. Instrum. Meas.* **2008**, *57*, 577−583.
(4) Banna, M. H.; Najjaran, H.; Sadiq, R.; Imran, S. A.; Rodriguez, M. J.; Hoorfar, M. Miniaturized water quality monitoring pH and conductivity sensors. *Sens. Actuators, B* **2014**, *193*, 434−441.
(5) Seyssiecq, I.; Veesler, S.; Boistelle, R. A non-immersed induction conductivity system for controlling supersaturation in corrosive media: the case of gibbsite crystals agglomeration in Bayer liquors. *J. Cryst. Growth* **1996**, *169*, 124−128.
(6) Browne, G. R.; Finn, C. W. P. The effects of aluminum content, temperature and impurities on the electrical conductivity of synthetic bayer liquors. *Metall. Trans. B* **1981**, *12*, 487−492.
(7) O'Brien, T. F.; Bommaraju, T. V.; Hine, F. Handbook of Chlor-Alkali Technology; *Developments in Hydrobiology*; Springer: Dordrecht, 2007.
(8) Tokuda, H.; Tsuzuki, S.; Susan, M. A. B. H.; Hayamizu, K.; Watanabe, M. How ionic are room-temperature ionic liquids? An indicator of the physicochemical properties. *J. Phys. Chem. B* **2006**, *110*, 19593−19600.
(9) Noda, A.; Hayamizu, K.; Watanabe, M. Pulsed-Gradient Spin−Echo 1 H and 19 F NMR Ionic Diffusion Coefficient, Viscosity, and Ionic Conductivity of Non-Chloroaluminate Room-Temperature Ionic Liquids. *J. Phys. Chem. B* **2001**, *105*, 4603−4610.
(10) Kreuer, K.-D. Proton Conductivity: Materials and Applications. *Chem. Mater.* **1996**, *8*, 610−641.
(11) Hapiot, P.; Lagrost, C. Electrochemical reactivity in room-temperature ionic liquids. *Chem. Rev.* **2008**, *108*, 2238−2264.
(12) Villar-Cociña, E.; Valencia-Morales, E.; González-Rodríguez, R.; Hernández-Ruíz, J. Kinetics of the pozzolanic reaction between lime and sugar cane straw ash by electrical conductivity measurement: A kinetic−diffusive model. *Cem. Concr. Res.* **2003**, *33*, 517−524.
(13) Brabants, G.; Hubin, M.; Reichel, E. K.; Jakoby, B.; Breynaert, E.; Taulelle, F.; Martens, J. A.; Kirschhock, C. E. A. Revisiting Silicalite-1 Nucleation in Clear Solution by Electrochemical Impedance Spectroscopy. *Langmuir* **2017**, *33*, 2581−2589.
(14) *Datasheet Memosens CLS82D conductivity sensor*; Endress +Hauser GmbH+Co., KG.
(15) *Datasheet InPro7000-VP/ InPro7100-VP conductivity sensors*; Mettler-Toledo AG.
(16) Ghosh, A. K. *Introduction to measurements and instrumentation*; Phi Learning: 2009.
(17) Doppelhammer, N.; Pellens, N.; Kirschhock, C. E.A.; Jakoby, B.; Reichel, E. K. Using Moving Electrode Impedance Spectroscopy to Monitor Particle Sedimentation. *IEEE Sens. J.* **2020**, 1.
(18) Lvovich, V. F. *Impedance Spectroscopy*; John Wiley & Sons, Inc: Hoboken, NJ, USA, 2012.
(19) Bach, H.; Baucke, F. G. K.; Krause, D. *Electrochemistry of Glasses and Glass Melts, Including Glass Electrodes*; Schott Series on Glass and Glass Ceramics, Science, Technology, and Applications; Springer: Berlin, Heidelberg, 2001.
(20) GILLIAM, R.; GRAYDON, J.; KIRK, D.; THORPE, S. A review of specific conductivities of potassium hydroxide solutions for various concentrations and temperatures. *Int. J. Hydrogen Energy* **2007**, *32*, 359−364.
(21) Vila, J.; Ginés, P.; Pico, J. M.; Franjo, C.; Jiménez, E.; Varela, L. M.; Cabeza, O. Temperature dependence of the electrical conductivity in EMIM-based ionic liquids. *Fluid Phase Equilib.* **2006**, *242*, 141−146.
(22) ASM International. *Fatigue data book: light structural alloys*; Materials Park, OH, 1995.
(23) Hamer, W. J.; DeWane, H. J. Electrolytic conductance and the conductances of the halogen acids in water; NSRDS-NBS, 33, 1970. DOI: 10.6028/NBS.NSRDS.33
(24) van Tendeloo, L.; Haouas, M.; Martens, J. A.; Kirschhock, C. E. A.; Breynaert, E.; Taulelle, F. Zeolite synthesis in hydrated silicate ionic liquids. *Faraday Discuss.* **2015**, *179*, 437−449.

https://dx.doi.org/10.1021/acssensors.0c01465
ACS Sens. 2020, 5, 3392−3397